PHOTOMETRY OF LONG-PERIOD ALGOL BINARIES. III. THE ACCRETION DISK AND MASS TRANSFER IN RZ OPHIUCHI

EDWARD C. OLSON
Astronomy Department, University of Illinois, Urbana, Illinois 61801
Received 18 May 1987; revised 17 July 1987

ABSTRACT

Five-color photometric observations of RZ Oph have been obtained from 1981 through 1986, in an effort to deduce the properties of the accretion disk in this long-period Algol. The partial eclipse of the disk by the cool star, and the partial occultation of the cool star by the disk, have both been observed in some detail. A simple gravitationally stratified model of the disk accounts very well for the emitted flux. The disk is viewed nearly edge-on, and is of moderate optical thickness. The principal extinction source in the disk is Rayleigh scattering from neutral hydrogen, and H^- contributes to the thermal absorption. Disk temperatures run from about 5600 K to about 4400 K at the edge of the disk, and the disk appears to overflow the Roche lobe of the hot star. Most of the disk's luminosity is supplied by gravitational accretion, implying a mass-transfer rate $\lesssim 10^{-6}\ \mathscr{M}_{\odot}$/yr. Brightness fluctuations of the disk seem to account for small intrinsic scatter that is present in the observations at most phases.

I. INTRODUCTION

The totally eclipsing long-period Algol binary RZ Ophiuchi (BD $+07°3832$; F5 Ib + K5 Ib; $P = 262$ days) has been studied for about 80 yr. Baldwin (1978) summarized the early work on this system. Circumstellar hydrogen line emission is present throughout the orbital cycle, though neither star is now thought to fill its Roche lobe. Hall (1969) associated an ultraviolet excess in primary eclipse with uneclipsed circumstellar light. Naftilan (1975) compared observed and synthetic spectra outside and in primary-eclipse totality, and found that both components appear to belong to luminosity class II and to have normal abundances. Baldwin (1978) derived spectroscopic and photometric elements, and deduced the presence of an extensive flattened disk around the hot star. The velocity structure in the disk was asymmetrical and non-Keplerian, and a lower mass limit of $\approx 10^{-10}\ \mathscr{M}_{\odot}$ was found. Smak (1981a) suggested that, if the orbital inclination were relaxed from 90° to about 75°, then the cool star could fill its Roche lobe. A number of objections were raised to this suggestion (Olson and Hickey 1983, hereafter referred to as OH; Forbes and Scarfe 1984; Knee *et al.* 1986). At the suggestion of Smak (1981b), several investigators recently obtained observations of RZ Oph (Papousek and Vetesnik 1982; van Paradijs, van der Woerd, van de Bis, and Van Suu 1982, hereafter referred to as VP; OH; Forbes and Scarfe 1984; Knee *et al.* 1986). Reliable geometrical elements are now available. Neither star can be more luminous than a giant, and the hot star may be close to the main sequence, but its light is contaminated by the surrounding disk. Partial eclipses of that disk produce depressions in the light curves around primary stellar eclipse. VP obtained excellent five-color Walraven photometry of these depressions in the 1981 eclipse. The partial disk eclipse prior to stellar eclipse was the steeper of the two, which these workers attributed to a hotspot on the trailing portion of the disk. OH discussed *uvby* photometry obtained at about the same time, and roughly analyzed the disk flux to find a disk temperature near 5000 K, and the presence of Rayleigh scattering from neutral hydrogen as the major source of disk extinction. Thanks to Forbes and Scarfe (1984) and Knee *et al.* (1986), we have a good double-line spectrographic solution, and a photometric solution that lacks only the explicit recognition of disk light and other circumstellar effects. The fractional radii of the hot and cool star are, respectively, $r_1 = 0.017 \pm 0.002$ and $r_2 = 0.128 \pm 0.016$, and the inclination $i = 90° \pm 3°$. The stellar separation is $a \sin i = (2.21 \pm 0.02) \times 10^{13}$ cm, and the mass ratio is $\mathscr{M}_2/\mathscr{M}_1 = 0.12 \pm 0.01$.

The present paper is the result of a multiyear effort to obtain *uvbyI* light curves that delineate clearly the photometric effects of the accretion disk.

II. OBSERVATIONS

It has been apparent almost from the start that photometric effects produced by the accretion disk in RZ Oph are small; i.e., $\lesssim 0.15$ mag. Only differential photometry of the highest precision and consistency could lead to success in this effort. All of the photometry reported in this paper was obtained at the Mount Laguna Observatory of San Diego State University. At 1860 m (6100 ft) elevation, this is an excellent site with high and stable transmission and dark skies. In 1981 and early 1982, *uvby* observations were made with the 0.4 m reflector. Beginning in October 1982, the Prairie 1 m reflector was used for *uvbyI* (Kron) photometry. All observations were made with the same filters, which, as noted below, were extremely stable throughout this interval. The observing season for RZ Oph coincides with the consistently best weather at Mount Laguna, which shares its weather cycle with the Palomar and Mount Wilson Observatories.

Observational procedures are described in Olson and Stoehr (1986). The comparison star was HD 173400 ($=$ BD $+06°3917$; G0). Its mean colors, derived from 13 nights when standards were also observed, are: $(b-y) = 0.422 \pm 0.002$; $(v-y) = 1.040 \pm 0.005$; $(u-b) = 1.703 \pm 0.004$; and $(V-I) = 0.505 \pm 0.021$. These are normal, essentially unreddened, indices for an F8 to G0 giant. The comparison star was checked on 31 nights against HD 173420 ($=$ BD $+06°3918$; K0) and was found to be constant to better than 0.005 mag in all colors. Check-star colors are also consistent with the spectral classification. All comparison/check observations were reduced on the natural system and corrected for (very small) differential extinction. The constancy of such checks for RZ Oph and for

 0004-6256/87/051309-09$00.90

a number of other binaries, where comparison and check stars differ appreciably in spectral type, proves the stability of the filters and the photometric systems during this period (see also Olson 1987a). When observations of RZ Oph were finished, all data were rereduced using the best mean transformation coefficients determined from many nights of standard-star observations during these several years. The photometry is therefore standardized, and stable to a few millimagnitudes. Observations of RZ Oph were made on parts of 89 nights from 1981 to 1986.* From times of primary minimum given by Baldwin (1978), Forbes and Scarfe (1984), and Knee *et al.* (1986), the following ephemeris is adopted: JD(hel.) pr. ecl. = 2,442,204.39 + 261.915 E. To give a general overview of light curves, these observations were averaged into bins of phase width 0.002 in primary stellar eclipse, 0.02 in secondary eclipse, and 0.023 outside eclipses. Resulting light curves are shown in Fig. 1. Except in the infrared, no observations are shown in primary stellar eclipse. The scatter in these light curves is mostly from real cycle-to-cycle variation. Light circles are *uvby* observations after primary eclipse in 1981, when these portions of the light curves were depressed by as much as 0.05 mag in *y*. OH discussed a possible reason for these depressions. Later observations in this part of the orbital cycle were, unfortunately, not numerous, but by 1984 this depression had apparently disappeared.

In all observations just prior to primary eclipse, a small but well-defined dip is present. This dip is produced when the large, cool star partially eclipses the leading edge of the accretion disk that surrounds the hot star. Arrows show the phases where disk eclipses would begin, if the disk filled the Roche lobe of the hot star, and if $i = 90°$. Near the beginning of this disk eclipse, light losses are more obvious at long wavelength. Later, toward first stellar contact at phase 0.977, disk light losses accelerate rapidly toward short wavelength. OH have already speculated that this light is from the hot star, and scattered mainly by Rayleigh scattering in the disk. OH did a preliminary analysis of the eclipsed disk light. The present paper analyzes this disk light in greater detail (Sec. V). As VP and OH had found, the disk eclipse is much less obvious after than before primary stellar eclipse. This point is discussed in Sec. V.

The most surprising feature of these curves is the prominent secondary eclipse, most obvious in the infrared, and giving that light curve an almost "W UMa-like" appearance (in a 262 day binary). Theoretical light curves calculated by assuming that all the light is stellar are superimposed on the infrared, yellow, blue, and violet light curves. These light curves were calculated with the Wilson-Devinney (WD) program (Wilson and Devinney 1971), using the geometrical elements of Knee *et al.* (1986). Similar light curves, synthesized using the WINK program (Wood 1972), gave interaction effects (mainly the tidal distortion of the cool star) that were appreciably smaller than those of WD. The latter is preferred, since it uses accurate Roche potentials. It appears that the accretion disk around the hot star absorbs and scatters much of the light of the cool star in and near secondary eclipse. The increase of the cool star's luminosity toward long wavelengths accounts for much of the prominence of secondary eclipse in the infrared. We are thus presented with the opportunity to probe both the emitting and the absorbing and scattering properties of the accretion disk in RZ Oph.

*All observations have been placed in the IAU Commission 27 Archives (Breger 1985) as file No. 203.

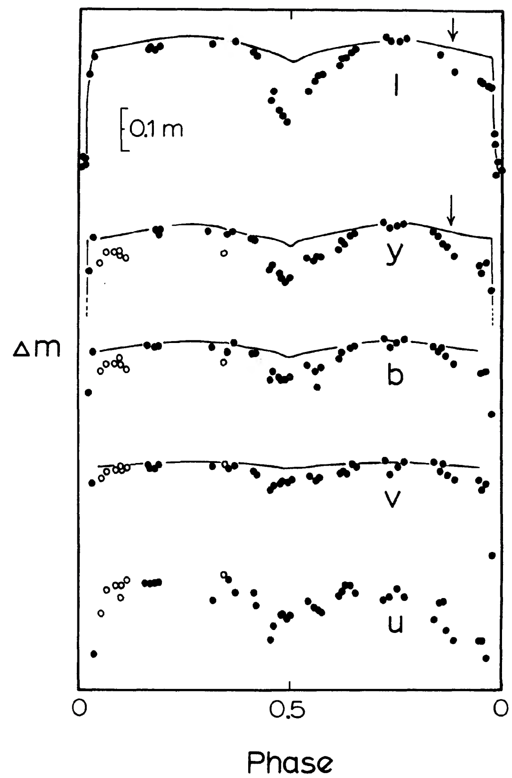

FIG. 1. Binned normal points of the approximately 5500 *uvbyI* observations of RZ Oph. Light circles are observations after primary eclipse, made in 1981. Solid curves are theoretical light curves, found by assuming that all the light is stellar. Vertical arrows mark the beginning of an eclipse of a disk just filling the Roche lobe of the hot star, if $i = 90°$.

While Fig. 1 gives a general impression of the light curves, it does not correctly show the relative magnitude scatter at different wavelengths. In Fig. 2, we plot four-point running normals on an expanded magnitude scale at the two wavelength extremes, and between phases 0.3 and external stellar contact. On this magnitude scale, scatter is large in the ultraviolet. To avoid large photon-statistical errors, each ultraviolet observation consisted of two or three 10 s counts, to bring the total count to about 10 000, where the statistical error is 0.01 mag. Most of the ultraviolet scatter in Fig. 2 is therefore real. However, the systemic light itself is faint in the ultraviolet, and the corresponding monochromatic flux scatter is not large enough to invalidate later analysis of these fluxes. None of the observations shown in Fig. 2 is in stellar primary eclipse. The rapid increase in light loss toward first stellar contact, noted above, is obvious in this figure. The effect is essentially absent in the infrared, but clearly present in the ultraviolet. It can also be seen in the blue and violet normals in Fig. 1. It will be argued below that hot-star light, Rayleigh scattered in the inner regions of the disk, is the cause of this behavior. The disk therefore has two sources: a thermal-emission component and a scattered-light component. The sum of both components yields flux L_λ (disk + s), while the thermal part alone is L_λ (disk). The components are relatively easy to separate in the light curves of disk eclipse.

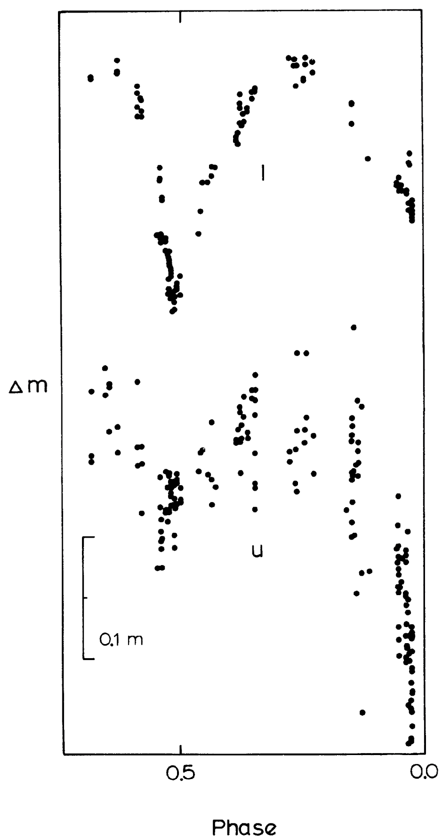

FIG. 2. Four-point running normals of infrared and ultraviolet observations between phases 0.3 and first contact of primary stellar eclipse. No observations in primary stellar eclipse are included. Secondary eclipse is produced mainly by a partial occultation of the cool star by the accretion disk. A partial eclipse of the disk by the cool star begins near phase 0.8.

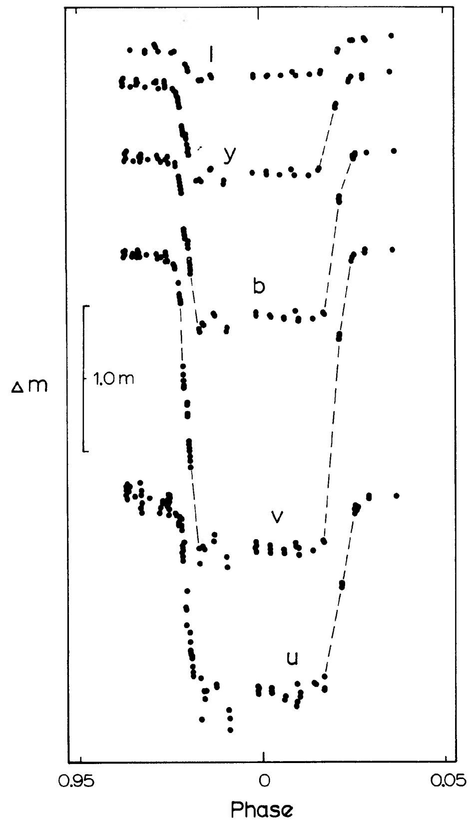

FIG. 3. Four-point running normals of primary stellar eclipse. No attempt was made to achieve complete coverage. The relative shallowness of ultraviolet eclipse is one indication of the presence of contaminating disk light in totality.

Four-point normals in primary stellar eclipse are shown in Fig. 3. Coverage is far from complete; that was not our objective. It is adequate to show clearly the variation of eclipse depth with wavelength. The relatively shallow ultraviolet eclipse is an indication that circumstellar light seriously contaminates totality. Moreover, totality tilts upward toward later phases at all wavelengths, suggesting that the circumstellar light eclipsed before is brighter than that eclipsed after mid-totality. This property is consistent with the weakness of the post-primary-eclipse dip. It is obvious that stellar and disk lights will have to be found, and a reasonable first approximation is that most of the disk light comes from its leading hemisphere.

III. DISK LIGHT

Figure 4 shows the geometry of RZ Oph, as viewed from above the orbital plane. The stars are fixed, and the observer revolves in the clockwise sense around the hot star. The disk around the hot star extends to, or even somewhat beyond, the Roche lobe. The leading half of the disk is the lower half in this figure. Horizontal sight lines correspond to mid-primary eclipse. The disk light still visible at mid-eclipse comes mainly from the lower sector of the disk. If, near this sector,

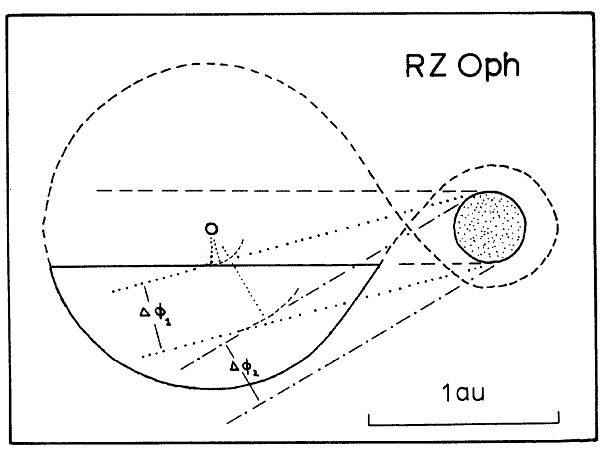

FIG. 4. The RZ Oph system, viewed from above the orbital plane. The observer is assumed to revolve around the small hot star in the clockwise direction. The accretion disk fills (possibly overfills slightly) the Roche lobe of the hot star, and the leading (lower) half of this disk is more luminous than the following half. Horizontal dashed lines are the lines of sight past the cool star at mid-primary eclipse. The disk light left at mid-eclipse comes mainly from the visible lower sector of the disk, marked out by full lines. This remaining disk light is approximately equal to the sum of the disk lights *lost* at phases $\Delta\phi_1$ and $\Delta\phi_2$, since roughly equal emitting volumes are involved in the disk light at mid-eclipse and at phases $\Delta\phi_1$ and $\Delta\phi_2$. Note that $\sin(\Delta\phi_1) = 2r_2$, and $\sin(\Delta\phi_2) = 4r_2$.

the disk light remains constant with azimuth, then the disk light visible at mid-eclipse can easily be found, as shown in Fig. 4. Let $\Delta\phi$ be the phase angle from mid-eclipse, and r_1 and r_2 be the fractional radii of the hot and cool star, respectively. Their values are 0.017 and 0.128. Choose the reference light level as the mean of observations near phase 0.75, where the total light is visible. The disk light seen at mid-eclipse will then be the sum of the disk lights lost at phase angles given by $\sin(\Delta\phi) = 2r_2$ and $\sin(\Delta\phi) = 4r_2$, or at phases 0.959 and 0.914. Correcting totality light for this disk contamination leaves $L(2)$. Classical interactions, particularly the tidal distortion of the cool star, were calculated with the WD program, and used in a simple iterative procedure to find stellar and disk lights. In a similar way, the entire lights of the disk, with and without the scattered light of the hot star, are found. These lights are converted to relative monochromatic fluxes using calibrations of Olson (1982), and are corrected for reddening $E_{by} = 0.1$, the value found by OH. These fluxes are listed in Table I, and relevant flux ratios are given in Table II. In the yellow, stellar fluxes are roughly comparable, while the cool star dominates in the infrared. Light in the ultraviolet is dominated by the hot star and the disk. The last column of Table II shows that the disk contributes 79% of the light in primary-eclipse totality, helping to explain the relative shallowness of ultraviolet primary eclipse.

There are several checks on the validity of this procedure of separating disk and stellar lights. In column 3 of Table II, the fraction of the disk light, including scattering, visible during totality decreases toward short wavelength, because most of the Rayleigh-scattered light is eclipsed. The fraction of the thermal disk emission visible at the same time (column 4) is more nearly constant, and equal to 0.72 ± 0.02. This figure is essentially identical to the fractional area of the Roche lobe of the hot star visible in totality (see Fig. 4), even if, as observations seem to suggest, most of the disk luminosity comes from the leading hemisphere. This procedure must also yield reasonable stellar flux distributions; these derived distributions are shown, with estimated error spreads, in Fig. 5. The cool-star spectrum matches fluxes derived from colors of an M3 III star, and shown as triangles. While disagreeing somewhat with the K5 Ib assignment given by Baldwin (1978), this type does agree with a recent preliminary classification by Peters (1985). The absence of an ultraviolet anomaly in the cool-star flux suggests that the contaminating disk flux has been successfully removed. The hot star must be near the main sequence, according to the solution of Knee *et al.* (1986). The light of the hot star experiences some extinction in passing through the disk, and, compared to theoretical model atmosphere fluxes, is particularly deficient in the ultraviolet. The observed distribution will therefore be

$$L_\lambda(1) \approx F_\lambda(\text{stellar})\exp[-f\tau_\lambda(\text{disk})],$$

where $\tau_\lambda(\text{disk})$ is the radial optical thickness of the disk, and f depends on the inclination of the orbital plane. Excellent agreement with the observed hot-star fluxes is obtained if $T \approx 6800$ K, $\log g = 4.0$, and $f \approx 0.7$. Theoretical points are shown as circles in Fig. 5. The fractional transmission of the disk runs from 0.68 in the infrared through 0.51 in the violet to 0.16 in the ultraviolet. The temperature lies within the error spread given by Knee *et al.* (1986). Note that all monochromatic fluxes given in Table I are expressed relative to the observed yellow flux of the hot star, dimmed by the surrounding accretion disk. This means that the error in $f\tau_y(\text{disk})$ will propagate into the derived disk fluxes. An error in the assumed reddening will, of course, also alter these fluxes somewhat.

IV. "SECONDARY ECLIPSE" AND THE TRANSMISSION OF THE DISK

It was clear from Fig. 1 that secondary eclipse is mainly produced by a partial occultation of the cool star by the accretion disk around the hot star. The cool-star flux increases

TABLE I. Monochromatic fluxes in RZ Ophiuchi.*

Filter	L_λ (1)	L_λ (2)	L_λ(disk+s)†	L_λ (disk)‡
I	0.49 ± 0.05	2.28 ± 0.04	0.52 ± 0.04	0.52 ± 0.04
y	1.00 ± 0.04	1.17 ± 0.03	0.54 ± 0.03	0.43 ± 0.03
b	1.18 ± 0.05	0.63 ± 0.03	0.41 ± 0.04	0.24 ± 0.04
v	1.16 ± 0.05	0.14 ± 0.04	0.37 ± 0.04	0.15 ± 0.04
u	0.18 ± 0.01	0.02 ± 0.01	0.15 ± 0.01	0.09 ± 0.01

* At reference phase 0.75, and relative to the observed yellow flux of the hot star.
† With Rayleigh-scattered hot star light.
‡ Without scattered hot star light.

TABLE II. Flux ratio in RZ Ophiuchi.*

Filter	L_λ(disk+s) / L_λ(total)†	L_λ(2) / L_λ(total)	L_λ(disk+s,totality) / L_λ(disk+s)	L_λ(disk,totality) / L_λ(disk)	L_λ(disk+s,totality) / Light in totality
I	0.16	0.69	0.69	0.69	0.14
y	0.20	0.43	0.59	0.72	0.22
b	0.18	0.28	0.46	0.74	0.25
v	0.22	0.08	0.32	0.76	0.48
u	0.43	0.06	0.44	0.70	0.79

*Symbols as in Table I.
†L_λ (total) $= L_\lambda(1) + L_\lambda(2) + L_\lambda$ (disk + s).

rapidly toward long wavelengths (Table I), which accounts for the prominence of the eclipse at long wavelengths. We wish to analyze the occulted light to derive the mean disk transmission, but because of cycle-to-cycle variations, we cannot use all of the relevant data in Fig. 1. From May to July 1985, however, a series of observations was obtained from phase 0.34 to just past 0.50 that defines the eclipse reasonably well. Four-point running normals are shown in Figs. 6(a) and 6(b). Solid lines are light curves from a WD synthesis, assuming that all the light is stellar. These figures show the increase in intrinsic scatter toward short wavelengths, but fortunately enough observations were made to average out much of this variation. To estimate the occulting effect of the disk, the mean of the three normals near phase 0.37 was selected as the reference level, Δm(ref). The mean of observations between phases 0.47 and 0.485, Δm(sec), was chosen to typify disk eclipse. Then, at any wavelength,

$$(1-F_t)\left[\frac{L(2)}{L(\text{total})}\right] = 1 - 10^{-0.4[\Delta m(\text{sec}) - \Delta m(\text{ref})]},$$

where $(1-F_t)$ is the fraction of the cool-star light blocked by the disk, and $L(\text{total}) = L(1) + L(2) + L(\text{disk})$. F_t is, of course, a mean of extinction and geometrical factors. Its relative variation with wavelength will show the variation of the mean disk extinction. Using the observations in Fig. 6 and the ratio $L(2)/L(\text{total})$ from Table I, we find $(1-F_t)$ shown, with estimated error ranges, in Fig. 7. Observed errors increase rapidly toward short wavelengths because secondary eclipse becomes shallow, and because $L(2)/L(\text{total})$ decreases rapidly. Nevertheless, the fractional blocking is well defined in the infrared, yellow, and blue, and it is further clear that the continuous disk extinction increases toward short wavelength. This behavior is in at least qualitative agreement with the results of OH, who found that Rayleigh scattering from neutral hydrogen was an important extinction source. We next consider the disk luminosity itself, and later return to consider the implied fractional light blocking by the disk.

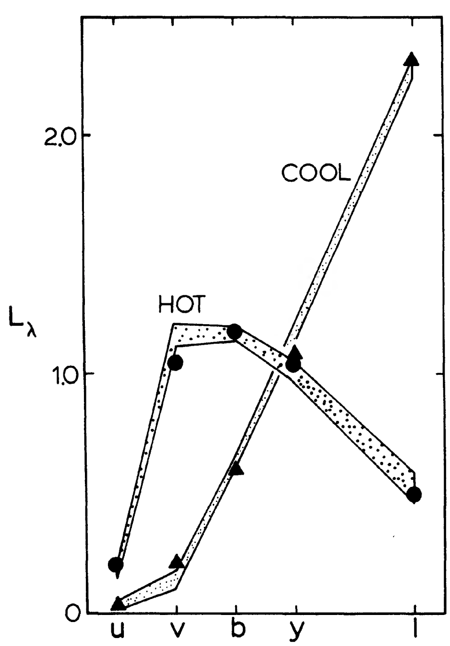

FIG. 5. Estimated flux distributions of hot and cool stars, after correcting for contaminating disk light. Symbols are best-matching single star fluxes. The normality of the cool-star flux suggests that the correction for disk light in totality is essentially correct. See the text for a discussion of the hot-star spectrum.

V. OBSERVATIONS OF, AND A MODEL FOR, THE DISK LIGHT

We have described the pre-primary-eclipse dip that begins in all colors near phase 0.80, and have suggested that it is caused by a partial eclipse of the leading edge of the accretion disk by the cool star. As before (OH), we express the monochromatic disk flux lost, relative to the yellow flux of the hot star, as L_λ (disk). The spectral distribution of this light well inside the dip is nonstellar and fairly red, in agreement with OH. It is crucial to verify that eclipsed disk light really is responsible for the dip in the light curve, as this light loss will be used below to estimate the accretional luminosity and the mass-transfer rate. Figure 8 shows monochromatic flux distributions for the light lost at three phases spread through the dip, found from the mean light curves. Their similar shapes suggest that only *one* light source is being eclipsed through the dip. A dip around primary eclipse might be pro-

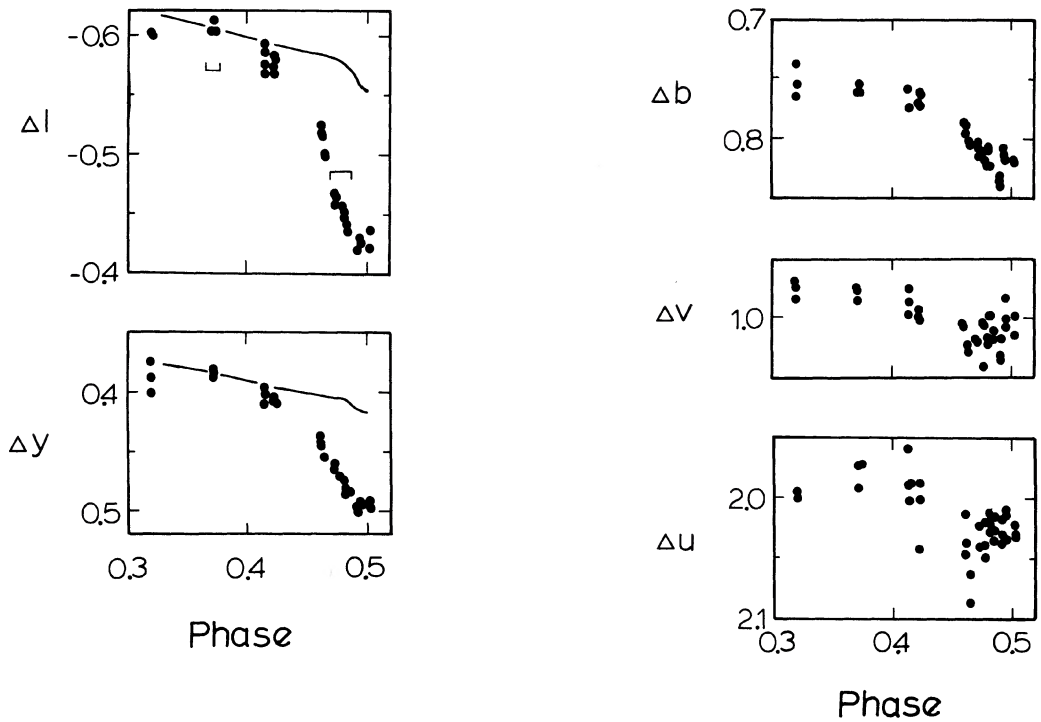

FIG. 6. Four-point running normals near and in secondary eclipse in 1985. Solid curves for I and y show calculated light curves, if all the light is stellar.

duced instead by an extended atmosphere around the cool star. Such an atmosphere might be an extreme case of the extended atmosphere found by Etzel and Olson (1985) around the cool component of S Cancri. This atmosphere would absorb and scatter hot-star light just outside external contacts of primary eclipse. A typical spectral distribution of such a light loss is shown as the dashed line in Fig. 8. No manipulation of parameters in the extended atmosphere can produce a distribution that resembles the observed one. However, the disk model described below gives theoretical fluxes shown as circles in Fig. 8. Their general agreement with observations strongly supports the origin of the dip in the partial eclipse of a disk by the cool star.

Figure 9 shows light curves of the partial disk eclipse. The speckled areas represent the thermal disk emission, while the dashed-line portions add the scattered hot-star light. The steep increase in the disk light toward external stellar contact, noted earlier, is particularly evident in the violet flux. This effect is smaller toward long wavelength, because less hot-star light is Rayleigh scattered by the inner regions of the disk. It is also smaller in the ultraviolet because there the flux of the hot star is much reduced. Since early attempts to model the disk light with a uniform emitting slab at constant temperature and pressure were promising, a somewhat more realistic model was developed. The geometry of this model is shown in Fig. 10. The hot star is at the coordinate origin, and the x-y plane is the orbital plane. The sight line of the observ-

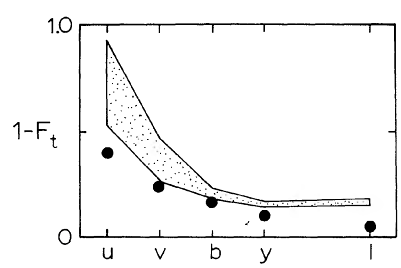

FIG. 7. The mean fractional transmission of the disk, with estimated errors, derived from the data in Fig. 6. The symbols are discussed in the text, in Sec. V.

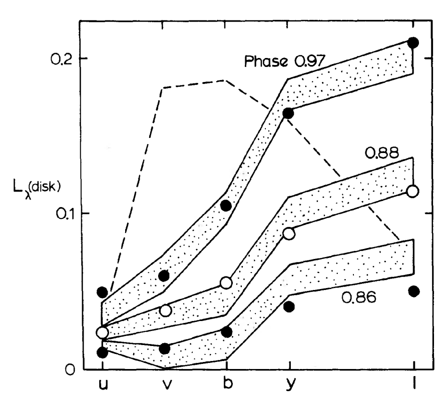

FIG. 8. Flux distributions of disk light lost at three phases in the disk eclipse. Symbols are model disk fluxes. The dashed line shows the distribution of a light loss produced instead, if an extended atmosphere around the cool star partially eclipses the hot star.

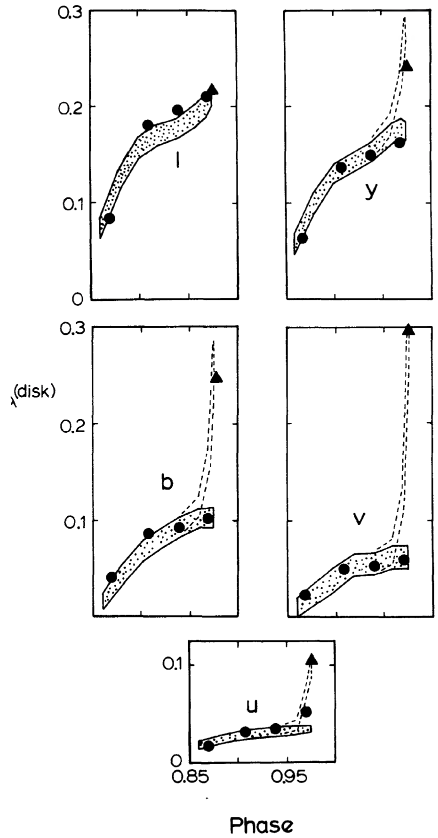

FIG. 9. Observed light curves of partial disk eclipse, with estimated error ranges (speckled areas). Symbols are from the disk model, discussed in Sec. V. Dashed lines include scattered hot-star light.

er at any phase within the disk eclipse is the y axis. The accretion disk is circular and azimuthally symmetric around the hot star within the leading half of the disk, and of radius R_D. The z component of the gravitational attraction of the hot star of mass $\mathscr{M}_1$ provides the vertical acceleration of gravity that stratifies the disk. For any point in the disk, this acceleration is

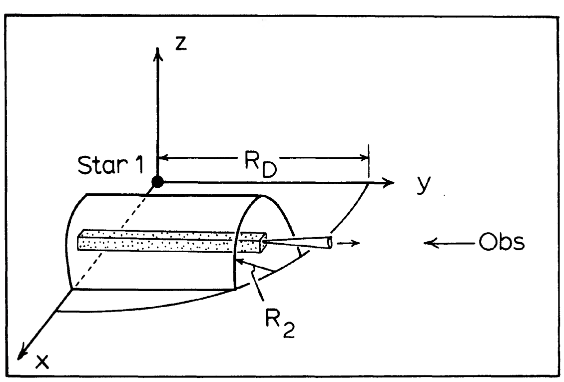

FIG. 10. Geometry of the disk model used to calculate the emitted disk flux and the fractional disk transmission. Only half of the light path through the disk is shown.

$$g_z = \frac{G\,\mathscr{M}_1 z}{(x^2+y^2+z^2)^{3/2}}.$$

Dropping the small z term leads to the usual simple result for the density:

$$\rho(x,y,z) \approx \exp\left[-Q(r)\frac{z^2}{(x^2+y^2)^{3/2}}\right].$$

Here

$$Q(r) = \frac{\mu m_H G\,\mathscr{M}_1}{2kT(r)}, \text{ and } r^2 = x^2 + y^2.$$

A radial central-plane temperature distribution $T(r)$ is introduced into the model. We do not use the analytical distribution for a steady-state α disk (Pringle 1981), because the disk in RZ Oph is optically thin in the vertical direction. Instead, we adopt the empirical distribution:

$$T(r) = T(RD) + [T(0) - T(RD)](1-r)^n,$$

where $T(0)$ is the extrapolated disk temperature at $r = 0$, and $T(RD)$ is the temperature at the outer edge of the disk. $T(r)$ is assumed to be constant with height z. $P(r)$ and $T(r)$ are related by assuming that $P \sim T^m$. No attempt, therefore, has yet been made to calculate a self-consistent disk model. We adopt the system parameters of Knee *et al.* (1986): $\mathscr{M}_1 = 1.1\times10^{34}$ g, $\mathscr{M}_2 = 1.4\times10^{33}$ g, $R_1 = 3.8\times10^{11}$ cm, $R_2 = 2.8\times10^{12}$ cm, $a = 2.2\times10^{13}$ cm, and $L_1 = 1.9\times10^{35}$ erg/s. Typical values for the disk in RZ Oph are: $\rho(r,0) \approx 3\times10^{-11}$ g/cm^3; $T \approx 5000$ K; vertical column density $\sigma_c \approx 50$ g/cm^2; and total extinction coefficient ≈ 0.001 cm^2/g. The disk light lost at any phase within the dip is found by integrating through the horizontal column of radius R_2 formed by sight lines that graze the periphery of the cool star. In the direction normal to the orbital plane, optical thicknesses are small. This means that once scattered, a photon is lost from the line of sight. Therefore, scattering contributes to the optical thickness along the line of sight, but not significantly to the source function, which we assume is thermal. Along any line of sight, the radiative-transfer equation is therefore

$$\frac{dI_\lambda}{(\kappa_\lambda + \sigma_\lambda)\rho\,dy} = -I_\lambda + \left(\frac{\kappa_\lambda}{\kappa_\lambda + \sigma_\lambda}\right)B_\lambda,$$

where all quantities have their usual meanings. The absence of scattering in the source function not only simplifies the calculation, but also helps, via Rayleigh scattering, to produce the very red color of the disk light. All quantities in the transfer equation are functions of position, and the contribution of any column to the disk light is simply

$$\int \kappa_\lambda \rho\, B_\lambda \, \exp[-t_\lambda(y)]\; dy,$$

where

$$t_\lambda(y) = \int_0^y (\kappa_\lambda + \sigma_\lambda)\rho\; dy.$$

Absorption and scattering coefficients were calculated in a subroutine extracted from ATLAS6 (Kurucz 1979), and modified for our use. Molecules are not included, but fortunately disk temperatures are just high enough, and pressures low enough, to preclude a significant molecular contribution. In practice, R_D, n, m, $T(0)$, $T(RD)$, and the "impact parameter" of the central sight line are assigned, and L_λ (disk) are calculated for a series of log $P(0)$, where $P(0)$ is the extrapolated central-plane pressure at the center of the disk. An upper limit for temperature is firmly set by the low disk ultraviolet flux, and therefore by the low value of the Balmer continuous absorption. Circles in Fig. 9 show results for $R_D = 5.9\ R(2)$, $n = 4$, $m = 2$, $T(0) = 5600$ K, $T(RD) = 4350$ K, and $\log P(0) = 1.1$. The disk mass $\approx 2 \times 10^{28}$ g or $\approx 10^{-5}\ \mathscr{M}_{\odot}$. No persistent effort was made to find a 'best' model, but it is evident that at most phases the disk light from the model is in reasonable agreement with observations. The model does not include light of the hot star that is Rayleigh scattered by the innermost regions of the disk; this omission is obvious in the disagreements in Fig. 9 near phase 0.975, just before external stellar contact. However, if we add an amount of light at this last phase that is proportional to $L_\lambda(1)/\lambda^4$, we get the triangles of Fig. 9. This Rayleigh contribution appears to remove the last obstacle to satisfactory agreement between observations and the model.

The outer disk radius R_D required to match observations implies that the accretion disk overflows the Roche lobe, at least above the leading hemisphere of the hot star, by about 30%. The amount of matter outside the Roche lobe is very small, however. Baldwin (1978) discussed the disk eclipse in Hβ, and found (his Figs. 7 and 8) the eclipse confined to ≈ 0.1 in phase from mid-primary eclipse. This corresponds to the emitting matter essentially filling the Roche lobe of the hot star. Disk eclipses prior to primary eclipse in Fig. 1 clearly start before phase 0.9, so apparently the outer regions of the disk do not emit Hβ. The large size of the disk is somewhat surprising and possibly questionable, but RZ Oph is not alone in this behavior. KU Cygni is a totally eclipsing binary with components similar to those in RZ Oph, but with a much shorter period of about 38 days. Its cool giant, unlike the one in RZ Oph, fills its Roche lobe. Both pre- and post-primary-eclipse dips are clearly present in KU Cyg, so an accretion disk is likely to be present around the hot star. This disk, too, appears to overflow the hot-star lobe (Olson 1987b).

VI. DISK LUMINOSITY AND POSSIBLE VARIATIONS

The observed disk luminosity, L_λ (disk), free of the scattered light of the hot star, is a measure of the accretional energy. To estimate the bolometric disk luminosity, we add to the disk fluxes in Table I fluxes found from the model to $\lambda \approx 20\,000$ Å. The bolometric disk flux is compared to the bolometric flux of the hot star, obtained from the hot-star fluxes of Table I, corrected for extinction by the disk, and to which are added theoretical infrared stellar fluxes. The ratio of bolometric disk to hot-star luminosities ≈ 0.33. How much of this disk luminosity is simply due to heating by the central star? The innermost part of the disk must be heated by the star (we have already identified and subtracted stellar scattered light from this region). With increasing distance r from the central star, the total disk thickness H increases as (Pringle 1981)

$$H/r = c_s/v_\phi \cong \text{const.}\sqrt{Tr},$$

where c_s is the sound speed in the disk, and v_ϕ is the circular disk speed. Toward the edge of the disk, H/r approaches 0.1, implying that the outer regions of the disk can intercept at most $\approx 0.05 L_1$. We estimate crudely that the disk luminosity, freed of stellar heating effects, is $\approx 0.2 L_1$, or 4×10^{34} erg/s. Assuming that the boundary layer adds a comparable amount, we estimate the total accretion luminosity at $\approx 0.8 \times 10^{35}$ erg/s, giving a mass-transfer rate $\approx 0.6 \times 10^{-6}\ \mathscr{M}_{\odot}$/yr. With a total disk mass $\approx 10^{-5}\ \mathscr{M}_{\odot}$, the mean particle disk residence time is about 17 yr.

The mass-transfer rate derived above for RZ Oph is very large to be supplied by a stellar wind from the cool giant companion, if that star is significantly smaller than its Roche lobe, as the best current model suggests (Fig. 4). Livio *et al.* (1986) have discussed accretion from stellar winds, and find for RZ Oph that the required wind velocity for disk formation is $\lesssim 3.8 \times 10^6$ cm/s. Disk formation from a wind is therefore marginally possible, though these authors suggest that it is more likely that the cool star is close to filling its Roche lobe, and that the wind is concentrated toward the hot star as described by Friend and Castor (1982). The orbital inclination of RZ Oph may therefore lie between values suggested by Smak (1981a) and Knee *et al.* (1986).

The problem of large mass flows from cool giants that fail to fill their Roche lobes is a recurrent one. An extensive program on SX Cassiopeiae, reported by Koch (1972), showed that secondary eclipse was much broader than primary eclipse, that a Rayleigh-scattering ring was present around the hot star, and that neither star approaches the inner contact surface. Plavec, Weiland, and Koch (1982) used *IUE* spectra to show that SX Cas is a Serpentid with considerable mass transfer and circumstellar matter. They also suggested that the wind from the cool giant may be amplified when the star is in a binary system. Kenyon and Gallagher (1983) commented on the same problem in symbiotics like AG Pegasi and CH Cygni. The difficulty has also been recently discussed by deKool, van den Heuvel, and Rappaport (1986).

The same program that calculates disk luminosities also finds the light blocking for use in secondary eclipse. Note that, since the disk is fully visible both before and within secondary eclipse, the occultation of the cool star by the disk is influenced only by extinction in the disk. That is, disk emission can be ignored. In Fig. 7, symbols show model-derived blocking fractions. At all stages of approximation, and in the final model, observed blocking fractions always exceeded calculated fractions, as though an extinction source, not contributing to re-emission in the visible, were present. The wavelength dependence of the inferred extinction does agree qualitatively with model extinction, and, except in the infrared, discrepancies are less than a factor of 2. Possibly, our estimate of extinction errors is too conservative, or departures from local thermodynamic equilibrium in the disk may account for the modest disagreement. It may be possible to check this point further in KU Cyg, and until analysis of that system is finished, we reserve judgment on the issue.

A significant fraction of the disk luminosity seems to originate from accretional energy. Viscous dissipation is a possible conversion mechanism, but relevant timescales must first be estimated. I thank Dr. Jim Pringle for emphasizing the importance of these times. The time to establish vertical hydrostatic equilibrium, $t_z \cong H/c_s$, is smaller than the disk rotation time, so hydrostatic equlibrium is a reasonable approximation. The thermal timescale for a steady-state viscous α disk (Shakura and Sunyaev 1983) is the internal energy divided by the dissipation rate, which can be expressed as $t_{th} \cong r/(v_\phi \alpha)$, and is roughly $10^6/\alpha$ s in the RZ Oph disk. In cataclysmic disks, $\alpha \lesssim 1$. If such viscous dissipation operates in RZ Oph, then t_{th} must be comparable to the radiative decay time of the disk, t_{rad} (as it is in cataclysmics). Since the disk is optically thin normal to the orbital plane,

$$t_{\rm rad} \cong \frac{3k}{8m_H \sigma_R \kappa T^3},$$

where σ_R is the Stefan-Boltzmann constant and κ the mean extinction coefficient. With $T \cong 5000$ K and $\kappa \cong 0.001$ $\mathrm{cm^2/g}$, $t_{\rm rad} \cong 5 \times 10^3$ s. This value is much smaller than $t_{\rm th}$, so the disk cannot be a viscous steady-state disk. Some other dissipative mechanism must convert gravitational to internal energy.

We noted that Fig. 2 shows a large increase in photometric scatter from infrared to ultraviolet. In secondary eclipse, as shown in Figs. 6(a) and 6(b), the scatter also increases from blue to ultraviolet. Observations in primary stellar eclipse (Fig. 3) show that during totality the scatter clearly increases, again from blue to ultraviolet. This is particularly evident just after second contact, where several normals form a small 'inverted-V' feature; the amplitude of this feature increases toward short wavelengths. To try to quantify these fluctuations, we consider only observations outside of all eclipses, which leaves just 12 nights' data. Fluctuations were not always present. Possibly by chance, observations near phase 0.75 (see Fig. 2) showed significant variations, while those near phase 0.2 showed little variation. Near phase 0.75 (38 observations in each color), the standard deviations per four-point normal were ± 0.007, ± 0.006, ± 0.009, ± 0.014, and ± 0.017 mag, from infrared to ultraviolet. Near phase 0.2 (34 observations per color), standard deviations were ± 0.004, ± 0.005, ± 0.001, ± 0.005, and ± 0.002 mag. Thus, when present, variations increased with decreasing wavelength. These variations were not anticipated, and the number of observations is really inadequate to demonstrate the properties of the variations. Future observations are planned with this objective in mind. We, of course, do not know the colors of these variations, but the fractional stellar and disk contributions to the total systemic light (Table II) clearly rule out the cool star as the source. The rather steep increase from infrared to violet of the hot-star contribution to total light rules against it as the source, leaving the disk itself. Table II shows the fractional disk contribution during totality; here, the disk must also be the source of the variations. If, therefore, there is only one source for all brightness fluctuations, then that source must be the accretion disk. (This situation contrasts with that in RS Cephei (Olson and Stoehr 1986; Olson 1986), an Algol with a period of 12.4 days. The disk in this system is faint, and intrinsic brightness variations were traced to the photosphere of the hot star. It was also possible to identify a few discrete accretion episodes when matter from the disk struck the photosphere of the hot star. Such accretion events have not yet been observed in RZ Oph. However, a preliminary analysis of KU Cyg shows that they do occur in this system.)

Disk-brightness variations might suggest that the disk is clumpy, and that dissipation occurs on a scale $\ll R_{\rm D}$. We would then observe a random superposition of dissipative events among the mass clumps, giving rise to the observed fluctuations. It is not clear why their visibility should depend on orbital phase.

A number of puzzles, beyond the nature of the dissipative mechanism, remain. The most obvious is the large light asymmetry between leading and following halves of the disk. The next opportunity to observe disk eclipse from start to finish occurs in the summer of 1989. We hope to observe this event, both photometrically and spectroscopically.

This research has been supported by the National Science Foundation under grants AST 80-24238 and 84-05319. The Research Board of the University of Illinois supported about half of the computational costs. This kind of long-term observing program, which also requires rather concentrated observing at certain phases, could not have been done at a national observatory. The author therefore especially thanks Dr. Burt Nelson, Director of the Mount Laguna Observatory, and Dr. Ron Angione and the staff of the Observatory for generous amounts of observing time and for much technical support. Drs. Ron Webbink, Mario Livio, Jim Pringle, Brian Warner, and Robert Wilson made a number of helpful suggestions. Many of the observations were made by Clayton Heller, Jeff Hickey, Linda Humes, Karen Kramer, and Victoria Paylor.

REFERENCES

Baldwin, B. W. (1978). Astrophys. J. **226**, 937.
Breger, M. (1985). Publ. Astron. Soc. Pac. **97**, 85.
Etzel, P. B., and Olson, E. C. (1985). Astron. J. **90**, 504.
Forbes, D., and Scarfe, C. D. (1984). Publ. Astron. Soc. Pac. **96**, 737.
Friend, D. B., and Castor, J. I. (1982). Astrophys. J. **261**, 293.
Hall, D. S. (1969). Bull. Am. Astron. Soc. **1**, 345.
Kenyon, S. J., and Gallagher, J. S. (1983). Astron. J. **88**, 666.
Knee, L. B. G., Scarfe, C. D., Mayor, M., Baldwin, B. W., and Meatheringham, S. J. (1986). Astron. Astrophys. **168**, 72.
Koch, R. H. (1972). Astron. J. **77**, 500.
deKool, M., van den Heuvel, E. P. J., and Rappaport, S. A. (1986). Astron. Astrophys. **164**, 73.
Livio, M., Soker, N., deKool, M., and Savonije, G. (1986). Mon. Not. R. Astron. Soc. **222**, 235.
Naftilan, S. A. (1975). Publ. Astron. Soc. Pac. **87**, 321.
Olson, E. C. (1982). Astrophys. J. **257**, 198.
Olson, E. C. (1986). Astron. J. **91**, 1421.
Olson, E. C. (1987a). In *New Generation Small Telescopes*, edited by D. Hayes, D. Genet, and R. Genet (Fairborn, Mesa, AZ) (to be published).
Olson, E. C. (1987b). In preparation.
Olson, E. C., and Hickey, J. P. (1983). Astrophys. J. **264**, 251.
Olson, E. C., and Stoehr, C. A. (1986). Astron. J. **91**, 1418.
Peters, G. J. (1985). Private communication.
Plavec, M. J., Weiland, J. L., and Koch, R. H. (1982). Astrophys. J. **256**, 206.
Pringle, J. E. (1981). Annu. Rev. Astron. Astrophys. **19**, 137.
Shakura, N. I., and Sunyaev, R. A. (1973). Astron. Astrophys. **24**, 337.
Smak, J. (1981a). Acta. Astron. **31**, 25.
Smak, J. (1981b). Inf. Bull. Var. Stars No. 1901.
van Paradijs, J., van der Woerd, H., van de Bis, M., and Van Suu, L. (1982). Astron. Astrophys. **111**, 372.
Wilson, R. E., and Devinney, E. J. (1971). Astrophys. J. **166**, 605.
Wood, D. P. (1972). Goddard Space Flight Center Rep. No. X-110-72-473 (Goddard Space Flight Center, Greenbelt, MD).